

The original version of this article has been published by Springer in Advances in Computational Mathematics, DOI 10.1007/s10444-007-9059-y, available at www.springerlink.com.

C^1 Hermite Interpolation by Pythagorean Hodograph Quintics in Minkowski space

Jiří Kosinka and Bert Jüttler*

*Johannes Kepler University, Institute of Applied Geometry, Altenberger Str. 69,
A-4040 Linz, Austria*

Abstract

Curves in the Minkowski space $\mathbb{R}^{2,1}$ are very well suited to describe the medial axis transform (MAT) of planar domains. Among them, Minkowski Pythagorean hodograph (MPH) curves correspond to domains where both the boundaries and their offsets admit rational parameterizations [4,13]. We construct MPH quintics which interpolate two points with associated first derivative vectors and analyze the properties of the system of solutions, including the approximation order of the ‘best’ interpolant.

Keywords: Hermite interpolation, Minkowski space, Minkowski Pythagorean hodograph curves.

1 Introduction

Pythagorean hodograph (PH) curves, which were introduced by Farouki and Sakkalis [9], admit rational parameterizations of their offsets (planar case) and low degree rational parameterizations of pipe surfaces (spatial case). PH curves and their applications have been thoroughly investigated, cf. [8,10,16] and the survey [7].

Minkowski Pythagorean hodograph (MPH) curves, which were introduced by Choi et al. and Moon [4,13], can be used to describe the segments of the

* Corresponding author.

Email addresses: {Jiri.Kosinka|Bert.Juettler}@jku.at.

medial-axis transform (cf. [6,14]) of a planar domain: if the medial axis transform is a collection of MPH curves, then the boundary curve of the associated planar domain is a piecewise rational curve. As an important advantage, this property is shared by all offsets of the boundary. Indeed, the offsetting operation corresponds to a special translation of the MAT in Minkowski space, which preserves the system of MPH curves.

The construction of PH and MPH curves is based on certain quadratic representation formulas which can be cast into a unifying framework, see [5]. Consequently, all methods for generating (M)PH curves from certain geometrical data require the solution of systems of quadratic equations. Since the computation and the analysis of solutions may become very involved for a large number of equations, the use of local constructions, which construct one segment of a PH/MPH curve at a time, appears to be the most promising approach. In particular, the construction of curves matching C^k or G^k Hermite boundary data has been addressed in the literature.

In the case of G^1 Hermite interpolation using PH cubics in \mathbb{R}^3 [10] or MPH cubics in $\mathbb{R}^{2,1}$ [11], there exist up to four interpolants. One of them possesses approximation order 4, provided that the data are taken from a curve without inflections. In the Minkowski case, that curve is assumed to be space-like.

The problem of C^1 Hermite interpolation with PH curves in \mathbb{R}^3 yields a two-parameter family of PH quintics [8,16]. There exists a particular interpolant which is geometrically invariant, preserves symmetry and planarity, and possesses approximation order 4.

A $C^{1/2}$ interpolation scheme using MPH quartics has been discussed in [12].

C^2 Hermite interpolation using PH curves of degree 9 in \mathbb{R}^3 gives a four-parameter family of interpolants [17]. The results are similar as in the C^1 case, but now with approximation order 6.

By using C^k data instead of G^k data, higher degrees of the interpolants are needed. On the other hand, the results about the approximation order are valid for a larger class of input curves. Moreover, while interpolants to G^k data exist only if certain solvability conditions are satisfied, no such constraints exist in the case of C^k data.

When comparing the results obtained in Euclidean and in Minkowski space, the latter space introduces some new phenomena. For instance, there exist curves with inflected segments in Minkowski space, which are not contained in straight lines. Additionally, points with light-like tangents cause problems and require a special treatment.

The remainder of the paper is organized as follows. In the following section

we recall some basic facts about the Minkowski space and its geometry, the Clifford algebra $\mathcal{C}(2, 1)$ and its use for representing MPH curves. The third section studies the problem of C^1 Hermite interpolation by MPH quintics and derives a parameterization of the family of interpolants. Section 4 identifies a particular solution. The fifth section analyzes the approximation order of this particular interpolant. Finally we present several examples and conclude this paper.

2 Preliminaries

In this section we summarize some fundamental concepts and results concerning Minkowski space, Lorentz transforms, Clifford algebras and MPH curves.

2.1 Minkowski space and Lorentz transforms

The three-dimensional *Minkowski space* $\mathbb{R}^{2,1}$ is a three-dimensional real affine space equipped with an indefinite inner product defined by the matrix

$$G = (G_{i,j})_{i,j=1,2,3} = \text{diag}(1, 1, -1). \quad (1)$$

The inner product of two vectors $\mathbf{u} = (u_1, u_2, u_3)^\top$, $\mathbf{v} = (v_1, v_2, v_3)^\top$ is

$$\langle \mathbf{u}, \mathbf{v} \rangle = \mathbf{u}^\top G \mathbf{v} = u_1 v_1 + u_2 v_2 - u_3 v_3. \quad (2)$$

As the quadratic form associated with G is not definite, the squared norm of a vector, which is defined by $\|\mathbf{v}\|^2 = \langle \mathbf{v}, \mathbf{v} \rangle$ can be positive, negative or zero. With a reference to the special theory of relativity, one distinguishes three ‘causal characters’ of vectors: A vector \mathbf{v} is said to be *space-like* if $\|\mathbf{v}\|^2 > 0$, *time-like* if $\|\mathbf{v}\|^2 < 0$, and *light-like* (or *isotropic*) if $\|\mathbf{v}\|^2 = 0$.

A *unit vector* $\mathbf{v} \in \mathbb{R}^{2,1}$ satisfies $\|\mathbf{u}\|^2 = \pm 1$. By scaling, space-like vectors \mathbf{u} can be normalized to satisfy $\|\mathbf{u}\|^2 = 1$, and time-like ones to satisfy $\|\mathbf{u}\|^2 = -1$.

A plane in Minkowski space is called *space-*, *time-* or *light-like* if the restriction of the quadratic form defined by G on this plane is positive definite, indefinite nondegenerate or degenerate, respectively.

A linear mapping $L : \mathbb{R}^{2,1} \rightarrow \mathbb{R}^{2,1}$ is called a *Lorentz transform* if it preserves the Minkowski inner product, i.e. $\langle \mathbf{u}, \mathbf{v} \rangle = \langle L\mathbf{u}, L\mathbf{v} \rangle$ for all $\mathbf{u}, \mathbf{v} \in \mathbb{R}^{2,1}$. The Lorentz transforms form the *Lorentz group* $\mathcal{L} = O(2, 1)$.

Any Lorentz transform is described by a 3×3 -matrix $L = (l_{i,j})_{i,j=1,2,3}$. Its column vectors \mathbf{l}_1 , \mathbf{l}_2 and \mathbf{l}_3 satisfy $\langle \mathbf{l}_i, \mathbf{l}_j \rangle = G_{i,j}$, $i, j \in \{1, 2, 3\}$, i.e., they

form an orthonormal basis of $\mathbb{R}^{2,1}$ with respect to the inner product (2). The equation $\langle \mathbf{l}_3, \mathbf{l}_3 \rangle = G_{3,3} = -1$ implies $l_{33}^2 \geq 1$. The Lorentz transform L is said to be *orthochronous* if $l_{33} \geq 1$. Obviously, the determinant of any Lorentz transform L equals to ± 1 . The *special* ones are characterized by $\det(L) = 1$.

The Lorentz group \mathcal{L} consists of four components. The special orthochronous Lorentz transforms form the subgroup $SO_+(2, 1)$. The remaining three components are $T_1 \cdot SO_+(2, 1)$, $T_2 \cdot SO_+(2, 1)$ and $T_1 \cdot T_2 \cdot SO_+(2, 1)$, where $T_1 = \text{diag}(1, 1, -1)$ and $T_2 = \text{diag}(1, -1, 1)$. Any special orthochronous Lorentz transform $L \in SO_+(2, 1)$ can be represented as $L = R(\alpha_1)H(\beta)R(\alpha_2)$, where

$$R(\alpha) = \begin{pmatrix} \cos \alpha & -\sin \alpha & 0 \\ \sin \alpha & \cos \alpha & 0 \\ 0 & 0 & 1 \end{pmatrix} \quad \text{and} \quad H(\beta) = \begin{pmatrix} 1 & 0 & 0 \\ 0 & \cosh \beta & \sinh \beta \\ 0 & \sinh \beta & \cosh \beta \end{pmatrix} \quad (3)$$

are a planar rotation with angle α , and a hyperbolic rotation (or ‘boost’) with angle β , respectively.

2.2 The Clifford algebra $\mathcal{C}(2, 1)$

Any real linear space, which is equipped with a non-degenerate quadratic form, has an associated Clifford algebra, see [5,15] for a more detailed introduction. In particular we are interested in the Clifford algebra $\mathcal{C}(2, 1)$, which corresponds to the Minkowski space $\mathbb{R}^{2,1}$, i.e., to the three-dimensional real linear space with the indefinite quadratic form (2).

This Clifford algebra has four different classes of basis elements: the *scalar* identity element $\mathbf{1}$, the orthonormal basis *vectors* $\mathbf{e}_1, \mathbf{e}_2, \mathbf{e}_3$, the *bivectors* $\mathbf{e}_{12}, \mathbf{e}_{23}, \mathbf{e}_{31}$ and the *pseudo-scalar* \mathbf{e}_{123} . The rules governing non-commutative multiplication \cdot can be deduced from the basic relations $\mathbf{e}_1^2 = \mathbf{e}_2^2 = \mathbf{1} = -\mathbf{e}_3^2$ and $\mathbf{e}_i \cdot \mathbf{e}_j = -\mathbf{e}_j \cdot \mathbf{e}_i$ if $i \neq j$.

Any element of the Clifford algebra is a linear combination of these basis elements. In order to simplify the notation, we shall use vectors in \mathbb{R}^8 to represent them,

$$\begin{aligned} A &= [a_0, a_1, a_2, a_3, a_4, a_5, a_6, a_7] = \\ &= a_0 \mathbf{1} + a_1 \mathbf{e}_1 + a_2 \mathbf{e}_2 + a_3 \mathbf{e}_3 + a_4 \mathbf{e}_{12} + a_5 \mathbf{e}_{23} + a_6 \mathbf{e}_{31} + a_7 \mathbf{e}_{123}. \end{aligned} \quad (4)$$

The *conjugation* of elements and the *squared norm* are defined as

$$\begin{aligned} \bar{A} &= [a_0, -a_1, -a_2, -a_3, -a_4, -a_5, -a_6, a_7] \quad \text{and} \\ N(A) &= A \cdot \bar{A} = (a_0^2 - a_1^2 - a_2^2 + a_3^2 + a_4^2 - a_5^2 - a_6^2 + a_7^2) + \\ &\quad + (2a_0 a_7 - 2a_1 a_5 - 2a_2 a_6 - 2a_3 a_4) \mathbf{e}_{123}, \end{aligned} \quad (5)$$

respectively. The operation of conjugation satisfies $\overline{A \cdot B} = \bar{B} \cdot \bar{A}$.

All vectors of $\mathbb{R}^{2,1}$ will be identified with *pure vectors*

$$\mathbf{c} = (\lambda, \mu, \nu)^\top \cong \lambda \mathbf{e}_1 + \mu \mathbf{e}_2 + \nu \mathbf{e}_3 = [0, \lambda, \mu, \nu, 0, 0, 0, 0] \in \mathcal{C}(2, 1). \quad (6)$$

The norms in $\mathbb{R}^{2,1}$ and $\mathcal{C}(2, 1)$ are related by

$$\|\mathbf{c}\|^2 = -N(\mathbf{c}) \quad (7)$$

The set of *scalars* combined with *bivectors* forms a subalgebra

$$\mathbb{H} = \mathbb{R}\mathbf{1} + \mathbb{R}\mathbf{e}_{12} + \mathbb{R}\mathbf{e}_{23} + \mathbb{R}\mathbf{e}_{31}. \quad (8)$$

of the Clifford algebra $\mathcal{C}(2, 1)$. Its elements will be represented by *calligraphic* characters, $\mathcal{A} = [a_0, 0, 0, 0, a_4, a_5, a_6, 0] = a_0\mathbf{1} + a_4\mathbf{e}_{12} + a_5\mathbf{e}_{23} + a_6\mathbf{e}_{31}$.

2.3 Solving certain quadratic equations in $\mathcal{C}(2, 1)$

We analyze the solutions of the equation

$$\mathcal{A} \cdot \mathbf{e}_1 \cdot \bar{\mathcal{A}} = \mathbf{c} \quad (9)$$

where \mathbf{c} is a pure vector and \mathcal{A} is an element of the subalgebra \mathbb{H} consisting of scalars and bivectors. Indeed, $\mathcal{A} \cdot \mathbf{e}_1 \cdot \bar{\mathcal{A}}$ is a pure vector if $\mathcal{A} \in \mathbb{H}$. At first we study the case where $\mathbf{c} = \mathbf{e}_1$.

Lemma 1 *All solutions of $\mathcal{W} \cdot \mathbf{e}_1 \cdot \bar{\mathcal{W}} = \mathbf{e}_1$ in the subalgebra \mathbb{H} form the four 1-parameter systems*

$$\begin{aligned} \mathcal{W}(1, \phi) &= [\cosh \phi, 0, 0, 0, 0, -\sinh \phi, 0, 0], & \phi \in \mathbb{R}, \\ \mathcal{W}(2, \phi) &= [-\cosh \phi, 0, 0, 0, 0, -\sinh \phi, 0, 0], & \phi \in \mathbb{R}, \\ \mathcal{W}(3, \phi) &= [0, 0, 0, 0, -\sinh \phi, 0, -\cosh \phi, 0], & \phi \in \mathbb{R}, \\ \mathcal{W}(4, \phi) &= [0, 0, 0, 0, -\sinh \phi, 0, \cosh \phi, 0], & \phi \in \mathbb{R}. \end{aligned} \quad (10)$$

These four systems can be identified with two hyperbolas in \mathbb{R}^8 .

Proof: The equation $\mathcal{W} \cdot \mathbf{e}_1 \cdot \bar{\mathcal{W}} = \mathbf{e}_1$, where $\mathcal{W} = [w_0, 0, 0, 0, w_4, w_5, w_6, 0]$, leads to

$$w_0^2 - w_4^2 - w_5^2 + w_6^2 = 1, \quad w_0 w_4 + w_5 w_6 = 0, \quad \text{and} \quad w_0 w_6 + w_4 w_5 = 0. \quad (11)$$

By forming the sum and difference of the last two equations, we obtain

$$(w_0 + w_5)(w_4 + w_6) = 0 \quad \text{and} \quad (w_0 - w_5)(w_4 - w_6) = 0. \quad (12)$$

Thus, we get $w_0 = \pm w_5$ and $w_4 = \pm w_6$ with four possible sign combinations. Substituting these results into the first equation yields

$$w_6^2 - w_4^2 = 1 \quad \text{or} \quad w_0^2 - w_5^2 = 1. \quad (13)$$

Consequently, the two hyperbolas (10) represent all solutions. \square

Remark 2 For the sake of brevity, we denote the ordered pair (i, ϕ) by $\bar{\phi}$, and we write $\mathcal{W}(\bar{\phi})$ instead of $\mathcal{W}(i, \phi)$. Moreover, the set of all solutions of $\mathcal{W} \cdot \mathbf{e}_1 \cdot \mathcal{W} = \mathbf{e}_1$ will be denoted by \mathbb{W} ,

$$\mathbb{W} = \{\mathcal{W}(i, \phi) : i = 1, \dots, 4; \phi \in \mathbb{R}\}. \quad (14)$$

Note that \mathbb{W} is centrally symmetric with respect to the origin $\mathbf{0}$, i.e., $\mathcal{W} \in \mathbb{W}$ implies $-\mathcal{W} \in \mathbb{W}$.

Lemma 3 *Let \mathbf{c} be a space-like vector in $\mathbb{R}^{2,1}$, which is identified with the corresponding element of the Clifford algebra. Let $\mathcal{A}, \mathcal{B} \in \mathbb{H}$ satisfy*

$$\mathcal{A} \cdot \mathbf{e}_1 \cdot \bar{\mathcal{A}} = \mathbf{c} = \mathcal{B} \cdot \mathbf{e}_1 \cdot \bar{\mathcal{B}}. \quad (15)$$

Then there exists a $\mathcal{W} \in \mathbb{W}$ such that $\mathcal{A} = \mathcal{B} \cdot \mathcal{W}$.

Proof: By taking the squared norm of the equation $\mathcal{B} \cdot \mathbf{e}_1 \cdot \bar{\mathcal{B}} = \mathbf{c}$ we obtain $N(\mathcal{B}) = \mathcal{B} \cdot \bar{\mathcal{B}} = \pm \sqrt{\|\mathbf{c}\|^2}$. On the other hand, by multiplying

$$\mathcal{A} \cdot \mathbf{e}_1 \cdot \bar{\mathcal{A}} = \mathcal{B} \cdot \mathbf{e}_1 \cdot \bar{\mathcal{B}} \quad (16)$$

with $\bar{\mathcal{B}}/\sqrt{\|\mathbf{c}\|^2}$ from the left-hand side and with $\mathcal{B}/\sqrt{\|\mathbf{c}\|^2}$ from the right-hand side, we arrive at

$$\left(\frac{\bar{\mathcal{B}} \cdot \mathcal{A}}{\sqrt{\|\mathbf{c}\|^2}}\right) \cdot \mathbf{e}_1 \cdot \left(\frac{\bar{\mathcal{B}} \cdot \mathcal{A}}{\sqrt{\|\mathbf{c}\|^2}}\right) = \mathbf{e}_1. \quad (17)$$

Due to Lemma 1 there exists a $\mathcal{W}' \in \mathbb{W}$ with $\mathcal{W}' = (\bar{\mathcal{B}} \cdot \mathcal{A})/\sqrt{\|\mathbf{c}\|^2}$. Multiplying this equation with \mathcal{B} from the left-hand side gives $\mathcal{A} = \mathcal{B} \cdot (\pm \mathcal{W}')$, and the result follows from the central symmetry of \mathbb{W} . \square

Finally we characterize all solutions of (9) in \mathbb{H} of a space- or light-like vector.

Lemma 4 *Consider a space-like or light-like vector $\mathbf{c} = (\lambda, \mu, \nu)^\top$, which is identified with the corresponding element of the Clifford algebra, and let*

$$\alpha(\mathbf{c}) = \frac{1}{2}(\lambda + \sqrt{\|\mathbf{c}\|^2}). \quad (18)$$

If $\alpha(\mathbf{c}) > 0$, then all solutions of the equation $\mathcal{X} \cdot \mathbf{e}_1 \cdot \bar{\mathcal{X}} = \mathbf{c}$ in the subalgebra \mathbb{H} can be expressed as

$$\mathcal{X}(i, \phi) = \frac{1}{2\sqrt{\alpha(\mathbf{c})}}[\nu, 0, 0, 0, 0, -\mu, 2\alpha(\mathbf{c}), 0] \cdot \mathcal{W}(i, \phi), \quad (19)$$

where $\phi \in \mathbb{R}$, $i \in \{1, 2, 3, 4\}$. If $\alpha(\mathbf{c}) < 0$, then they can be expressed as

$$\mathcal{X}(i, \phi) = \frac{1}{2\sqrt{-\alpha(\mathbf{c})}}[0, 0, 0, 0, \nu, -2\alpha(\mathbf{c}), -\mu, 0] \cdot \mathcal{W}(i, \phi), \quad (20)$$

where again $\phi \in \mathbb{R}$, $i \in \{1, 2, 3, 4\}$.

Proof: If \mathbf{c} is space-like, then any of these solutions can be obtained by multiplying a particular solution with a suitable element of \mathbb{W} , see Lemma 3. A straightforward computation confirms that $\mathcal{X}(i, 0)$ gives indeed a particular solution. On the other hand, if \mathbf{c} is light-like, then the result of that Lemma cannot be used. However, a direct computation (similar to the one in Lemma 1) confirms that the formulas (19) and (20) represent all solutions. \square

Remark 5 If $\alpha(\mathbf{c}) = 0$, i.e. if $\lambda \leq 0$ and $\mu^2 = \nu^2$, one obtains different 1-parametric families of solutions. This is due to the fact that the particular solution cannot be computed using Lemma 4. This is similar to [8, Eq. (22) and Footnote 4]. Geometrically, this occurs when \mathbf{c} lies in one of the two half-planes obtained as bisectors of the μ and ν axes, restricted to the half-space $\lambda \leq 0$. We exclude this case from our considerations. This is just a technical assumption, which we make in order to simplify the presentation. As we shall see later in Section 5, the case $\alpha(\mathbf{c}) = 0$ does not occur if the data are sampled from a space-like C^∞ curve with sufficiently small step-size.

2.4 MPH curves

Recall that a polynomial curve in Euclidean space is called a *Pythagorean hodograph* (PH) curve (cf. [7]), if the squared norm of its first derivative (or hodograph) is the square of another polynomial. Following [13], *Minkowski Pythagorean hodograph* (MPH) curves are defined similarly, but with respect to the norm induced by the Minkowski inner product. More precisely, a polynomial curve $\mathbf{c} \in \mathbb{R}^{2,1}$, $\mathbf{c} = (x, y, r)^\top$ is called an MPH curve if

$$\|\mathbf{c}'\|^2 = x'^2 + y'^2 - r'^2 = \sigma^2 \quad (21)$$

for some polynomial σ .

As observed in [4,13], if the medial axis transform (MAT) of a planar domain is (a collection of) MPH curve(s), then the coordinate functions of the corresponding boundary curves (i.e., the envelopes of the circles with centers (x, y)

and radius r) are (piecewise) rational functions. For instance, if (x, y, r) is an MPH quintic, then the boundaries are rational curves of degree 13.

Due to the definition of MPH curves, the tangent vector $\mathbf{c}'(t)$ cannot be time-like. Also, light-like tangent vectors correspond to roots of the polynomial σ in (21). Each regular point of an MPH curve has a space-like or light-like tangent vector. It corresponds to two or to one point on the boundaries of the associated planar domain, respectively. See [14, Section 2.1] for more information concerning the relation between general curves (not only MPH curves) in $\mathbb{R}^{2,1}$ and the boundaries of the associated planar domain.

According to [13], the equation (21) holds if and only if there exist polynomials $u(t)$, $v(t)$, $p(t)$ and $q(t)$ such that

$$\begin{aligned} x'(t) &= u(t)^2 - v(t)^2 - p(t)^2 + q(t)^2, \\ y'(t) &= -2(u(t)v(t) + p(t)q(t)), \\ r'(t) &= 2(u(t)q(t) + v(t)p(t)), \\ \sigma(t) &= u(t)^2 + v(t)^2 - p(t)^2 - q(t)^2. \end{aligned} \tag{22}$$

This result can be reformulated using Clifford algebra $\mathcal{C}(2, 1)$, see [5], by again identifying vectors with elements of the algebra, cf. (6).

Lemma 6 *A polynomial curve $\mathbf{p}(t)$ in $\mathbb{R}^{2,1}$ is an MPH curve if and only if there exists a polynomial curve $\mathcal{A}(t) = u(t) + v(t)\mathbf{e}_{12} + p(t)\mathbf{e}_{23} + q(t)\mathbf{e}_{31}$ in the subalgebra \mathbb{H} such that*

$$\mathbf{p}'(t) = \mathbf{h}(t) = \mathcal{A}(t) \cdot \mathbf{e}_1 \cdot \bar{\mathcal{A}}(t) \tag{23}$$

holds.

Consequently, the construction of MPH curves is reduced to the construction of a suitable curve $\mathcal{A}(t)$ in the subalgebra \mathbb{H} , which will be called the *preimage* curve.

3 C^1 Hermite interpolation by MPH quintics

We construct MPH curves $\mathbf{p}(t)$ which match given C^1 Hermite boundary data. More precisely, the curves are to interpolate the boundary points

$$\mathbf{p}_0 = \mathbf{p}(0), \quad \mathbf{p}_1 = \mathbf{p}(1) \tag{24}$$

and the boundary tangent vectors

$$\mathbf{t}_0 = \mathbf{p}'(0), \quad \mathbf{t}_1 = \mathbf{p}'(1). \tag{25}$$

As a technical assumption, we exclude the cases $\alpha(\mathbf{t}_0) = 0$ or $\alpha(\mathbf{t}_1) = 0$, see Lemma 4 and Remark 5.

Two curves $\mathbf{p}(t)$, $\tilde{\mathbf{p}}(t)$ share the same hodograph if and only if they differ by a translation. Consequently, an MPH curve $\mathbf{p}(t)$ is uniquely determined by its preimage $\mathcal{A}(t)$ and its starting point $\mathbf{p}_0 = \mathbf{p}(0)$. The position of $\mathbf{p}(0)$ can be matched by a suitable choice of the integration constant. Thus, 9 interpolation conditions are to be satisfied by the control points of $\mathcal{A}(t)$.

We choose the degree of $\mathcal{A}(t)$ to be equal to 2, which gives 12 free parameters. Since the representation of Lemma 6 has one-dimensional fibers, we expect to obtain a 2 ($= 12 - 9 - 1$) – dimensional system of MPH interpolants of degree 5 ($= 2 \times 2 + 1$).

We express the hodograph $\mathbf{h}(t) = \mathbf{p}'(t)$ and the preimage $\mathcal{A}(t)$ by their Bernstein–Bézier representations,

$$\mathbf{h}(t) = \sum_{i=0}^4 \mathbf{h}_i B_i^4(t), \quad \mathcal{A}(t) = \sum_{i=0}^2 \mathcal{A}_i B_i^2(t), \quad t \in [0, 1], \quad (26)$$

where \mathbf{h}_i (vectors) and \mathcal{A}_i (scalars and bivectors) are the control points and $B_i^n(t) = \binom{n}{i} t^i (1-t)^{n-i}$ are the Bernstein polynomials. The interpolation conditions give the equations

$$\mathbf{h}_0 = \mathbf{t}_0, \quad \mathbf{h}_4 = \mathbf{t}_1, \quad \sum_{i=0}^4 \mathbf{h}_i = 5(\mathbf{p}_1 - \mathbf{p}_0), \quad (27)$$

which have to be satisfied by the control points of the hodograph. We express these equations in terms of the preimage control points. After a suitable re-arranging we arrive at the equations

$$\mathcal{A}_0 \cdot \mathbf{e}_1 \cdot \bar{\mathcal{A}}_0 = \mathbf{t}_0, \quad \mathcal{A}_2 \cdot \mathbf{e}_1 \cdot \bar{\mathcal{A}}_2 = \mathbf{t}_1 \quad (28)$$

and (note that $\mathcal{A}_0 \cdot \mathbf{e}_1 \cdot \bar{\mathcal{A}}_2 + \mathcal{A}_2 \cdot \mathbf{e}_1 \cdot \bar{\mathcal{A}}_0$ is a pure vector if $\mathcal{A}_0, \mathcal{A}_2 \in \mathbb{H}$)

$$\begin{aligned} & (3\mathcal{A}_0 + 4\mathcal{A}_1 + 3\mathcal{A}_2) \cdot \mathbf{e}_1 \cdot (3\bar{\mathcal{A}}_0 + 4\bar{\mathcal{A}}_1 + 3\bar{\mathcal{A}}_2) = \\ & = 120(\mathbf{p}_1 - \mathbf{p}_0) - 15(\mathbf{t}_1 + \mathbf{t}_0) + 5(\mathcal{A}_0 \cdot \mathbf{e}_1 \cdot \bar{\mathcal{A}}_2 + \mathcal{A}_2 \cdot \mathbf{e}_1 \cdot \bar{\mathcal{A}}_0) \end{aligned} \quad (29)$$

These three equations are of the form $\mathcal{A} \cdot \mathbf{e}_1 \cdot \bar{\mathcal{A}} = \mathbf{c}$, and they can therefore be solved with the help of Lemma 4, as follows.

Firstly, we compute the solutions $\mathcal{A}_0(i, \phi_0) = \mathcal{A}_0(\bar{\phi}_0)$ and $\mathcal{A}_2(k, \phi_2) = \mathcal{A}_2(\bar{\phi}_2)$ of (28) in the form of (19) or (20). Secondly, after substituting them into (29) and again solving the resulting equation, we obtain a 3-parametric system of control points $\mathcal{A}_1 = \mathcal{A}_1(\bar{\phi}_0, \bar{\phi}_1, \bar{\phi}_2)$. These control points depend on the parameters $\bar{\phi}_i \in \{1, 2, 3, 4\} \times \mathbb{R}$, $i = 0, 1, 2$.

Summing up, we arrive at a 3-parametric system of suitable preimages

$$\mathcal{A}[\bar{\phi}_0, \bar{\phi}_1, \bar{\phi}_2](t) = \mathcal{A}_0(\bar{\phi}_0) B_0^2(t) + \mathcal{A}_1(\bar{\phi}_0, \bar{\phi}_1, \bar{\phi}_2) B_1^2(t) + \mathcal{A}_2(\bar{\phi}_2) B_2^2(t). \quad (30)$$

The hodographs of the MPH interpolants are then obtained as

$$\mathbf{h}[\bar{\phi}_0, \bar{\phi}_1, \bar{\phi}_2](t) = \mathcal{A}[\bar{\phi}_0, \bar{\phi}_1, \bar{\phi}_2](t) \cdot \mathbf{e}_1 \cdot \bar{\mathcal{A}}[\bar{\phi}_0, \bar{\phi}_1, \bar{\phi}_2](t). \quad (31)$$

However, as in the Euclidean case (see [8,16]), one of the three parameters is redundant.

Lemma 7 *Let $\mathbf{h}[(i, \phi_0), (j, \phi_1), (k, \phi_2)](t)$ be the hodograph of a particular MPH interpolant to some given input data. Then there exist parameters ρ_0, ρ_2 and integers $p, q \in \{1, 2, 3, 4\}$ such that*

$$\forall t : \mathbf{h}[(i, \phi_0), (j, \phi_1), (k, \phi_2)](t) = \mathbf{h}[(p, \rho_0), (1, 0), (q, \rho_2)](t) \quad (32)$$

holds.

Proof: We consider the preimage control points $\mathcal{A}_0(i, \phi_0), \mathcal{A}_1(j, \phi_1), \mathcal{A}_2(k, \phi_2)$. For any value of the additional parameter $\theta \in \mathbb{R}$, we consider the ‘rotated’ preimage control points, which are obtained by changing the parameters to

$$(i, \phi_0 + (-1)^i \theta), \quad (j, \phi_1 + (-1)^j \theta), \quad \text{and} \quad (k, \phi_2 + (-1)^k \theta). \quad (33)$$

Due to the identity

$$\mathcal{W}(i, \phi + (-1)^i \theta) = \mathcal{W}(i, \phi) \cdot \mathcal{W}(1, -\theta), \quad i \in \{1, 2, 3, 4\}, \quad (34)$$

which is a direct consequence of the addition theorems for hyperbolic functions, one can verify that the new preimage control points are obtained by multiplying the original ones by $\mathcal{W}(1, -\theta)$ from the right-hand side. Let

$$\mathcal{P}(t) = \mathcal{A}[(i, \phi_0), (j, \phi_1), (k, \phi_2)](t) \quad (35)$$

and

$$\tilde{\mathcal{P}}(t) = \mathcal{A}[(i, \phi_0 + (-1)^i \theta), (j, \phi_1 + (-1)^j \theta), (k, \phi_2 + (-1)^k \theta)](t) \quad (36)$$

be the original and the rotated preimage, respectively. The corresponding hodographs satisfy

$$\tilde{\mathcal{P}}(t) \cdot \mathbf{e}_1 \cdot \bar{\tilde{\mathcal{P}}}(t) = \mathcal{P}(t) \cdot \mathcal{W}(1, -\theta) \cdot \mathbf{e}_1 \cdot \overline{\mathcal{P}(t) \cdot \mathcal{W}(1, -\theta)} = \mathcal{P}(t) \cdot \mathbf{e}_1 \cdot \bar{\mathcal{P}}(t), \quad (37)$$

i.e., we obtain the same MPH interpolant for any choice of θ . In particular, by choosing $\theta = (-1)^{j+1} \phi_1$, we find parameters $\rho_0 = \phi_0 + (-1)^i \theta$, $\rho_2 = \phi_2 + (-1)^k \theta$ such that

$$\forall t : \mathbf{h}[(i, \phi_0), (j, \phi_1), (k, \phi_2)](t) = \mathbf{h}[(i, \rho_0), (j, 0), (k, \rho_2)](t). \quad (38)$$

Next we observe that $\mathcal{W}(1, 0) = \mathbf{e}$, $\mathcal{W}(2, 0) = -\mathbf{e}$, $\mathcal{W}(3, 0) = -\mathbf{e}_{31}$ and $\mathcal{W}(4, 0) = \mathbf{e}_{31}$. Any one of these four Clifford algebra elements can be obtained

by multiplying one of them with all values of the set $\mathbb{E} = \{\mathbf{e}, -\mathbf{e}, \mathbf{e}_{31}, -\mathbf{e}_{31}\}$ from the right-hand side. Moreover, if we right-multiply the entire preimage by $\mathcal{E} \in \mathbb{E}$, i.e. $\tilde{\mathcal{P}}(t) = \tilde{\mathcal{P}}(t) \cdot \mathcal{E}$, then the hodograph remains unchanged, since

$$\tilde{\mathcal{P}}(t) \cdot \mathcal{E} \cdot \mathbf{e}_1 \cdot \overline{\tilde{\mathcal{P}}(t) \cdot \mathcal{E}} = \tilde{\mathcal{P}}(t) \cdot \mathbf{e}_1 \cdot \tilde{\mathcal{P}}(t). \quad (39)$$

Consequently, we can always right-multiply the preimage by a suitable $\mathcal{E} \in \mathbb{E}$ such that the index j of the middle parameter $\bar{\phi}_1$ becomes 1. \square

In the remainder of this paper we use the reduced set of free parameters and denote the preimages with

$$\mathcal{A}[\bar{\phi}_0, \bar{\phi}_2](t) = \mathcal{A}[(i, \phi_0), (1, 0), (k, \phi_2)](t) \quad (40)$$

The corresponding quintic MPH interpolants are

$$\mathbf{p}[\bar{\phi}_0, \bar{\phi}_2](\tau) = \mathbf{p}_0 + \int_0^\tau \mathcal{A}[\bar{\phi}_0, \bar{\phi}_2](t) \cdot \mathbf{e}_1 \cdot \bar{\mathcal{A}}[\bar{\phi}_0, \bar{\phi}_2](t) dt. \quad (41)$$

Among these solutions we identify a special one.

4 Identifying a particular solution

After analyzing the influence of some specific Lorentz transforms to the free parameters controlling the interpolant, we identify a geometrically invariant particular solution with certain symmetry properties. More precisely, the computation of the solution commutes with Lorentz transforms, translations and reversion of the data.

4.1 The parameterization of the interpolants and Lorentz transforms

For any given C^1 Hermite data $\mathbf{p}_0, \mathbf{p}_1, \mathbf{t}_0, \mathbf{t}_1$, the system

$$\{\mathbf{p}[\bar{\phi}_0, \bar{\phi}_2](t) : \bar{\phi}_0 = (i, \phi_0), \bar{\phi}_2 = (k, \phi_2), \phi_0, \phi_2 \in \mathbb{R}, i, k = 1, \dots, 4\} \quad (42)$$

represents *all* MPH interpolants. Therefore, it is invariant with respect to Lorentz transforms. More precisely, if we apply a Lorentz transform L to the Hermite data, we obtain modified data $\tilde{\mathbf{p}}_0 = L(\mathbf{p}_0)$, $\tilde{\mathbf{p}}_1 = L(\mathbf{p}_1)$, $\tilde{\mathbf{t}}_0 = L(\mathbf{t}_0)$, $\tilde{\mathbf{t}}_1 = L(\mathbf{t}_1)$, along with the modified interpolating MPH curves $\tilde{\mathbf{p}}[\bar{\psi}_0, \bar{\psi}_2](t)$. The systems of interpolants satisfy

$$\forall \bar{\phi}_0, \bar{\phi}_2 : \exists \bar{\psi}_0, \bar{\psi}_2 : \forall t : \tilde{\mathbf{p}}[\bar{\psi}_0, \bar{\psi}_2](t) = L(\mathbf{p}[\bar{\phi}_0, \bar{\phi}_2](t)). \quad (43)$$

In general, however, the transform L does not preserve the parameterization of

the interpolants by the free parameters $\bar{\phi}_i, \bar{\psi}_k$. The relations $\bar{\psi}_0 = \bar{\phi}_0, \bar{\psi}_2 = \bar{\phi}_2$ are not always satisfied.

In order to identify a particular solution which is geometrically invariant, we analyze the behavior of the free parameters under Lorentz transforms. We restrict ourselves to the so-called “main branch” of interpolants:

Definition 1 *We assume that the data are chosen such that the interpolants in (42) which are obtained by choosing $i = k = 1$ are computed solely by using the solutions (19). Under this assumption, these interpolants are said to form the **main branch** of interpolants. They will be denoted by $\mathbf{p}_0[\phi_0, \phi_2]$.*

As shown in the following sections, the main branch of MPH interpolants includes the one which is most useful.

Lemma 8 *We consider a solution of the main branch which is obtained for two arbitrary but fixed values $\phi_0, \phi_2 \in \mathbb{R}$.*

- 1) *If Ξ_1 is a hyperbolic rotation about the \mathbf{e}_1 axis and $\tilde{\mathbf{p}}_0$ the main branch of interpolants for the transformed data, then*

$$\forall t : \tilde{\mathbf{p}}_0[\phi_0, \phi_2](t) = \Xi_1(\mathbf{p}_0[\phi_0, \phi_2](t)). \quad (44)$$

- 2) *If Ξ_2 is a reflection with respect to a non-light-like plane containing the \mathbf{e}_1 axis, then*

$$\forall t : \tilde{\mathbf{p}}_0[-\phi_0, -\phi_2](t) = \Xi_2(\mathbf{p}_0[\phi_0, \phi_2](t)). \quad (45)$$

Proof: For arbitrary but fixed ϕ_0, ϕ_2 , let $\mathcal{A}_0, \mathcal{A}_1, \mathcal{A}_2$ be the control points of the preimage for some input data $\mathbf{p}_0, \mathbf{p}_1, \mathbf{t}_0, \mathbf{t}_1$, and $\tilde{\mathcal{A}}_0, \tilde{\mathcal{A}}_1, \tilde{\mathcal{A}}_2$ for the transformed input data.

Any hyperbolic rotation about the \mathbf{e}_1 axis through an angle θ (cf. (3)) can be represented by the mapping

$$\Xi_1([0, \lambda, \mu, \nu, 0, 0, 0, 0]) = [0, \lambda, \mu c + \nu s, \nu c + \mu s, 0, 0, 0, 0], \quad (46)$$

where $c = \cosh \theta$, $s = \sinh \theta$. We extend Ξ_1 to the entire Clifford algebra, except for the last coordinate,

$$\Xi_1([a_0, \lambda, \mu, \nu, a_4, a_5, a_6, 0]) = [a_0 c - a_5 s, \lambda, \mu c + \nu s, \nu c + \mu s, a_4, a_5 c - a_0 s, a_6, 0]. \quad (47)$$

Using (28) one can verify that

$$\tilde{\mathcal{A}}_0 = \Xi_1(\mathcal{A}_0) \text{ and } \tilde{\mathcal{A}}_2 = \Xi_1(\mathcal{A}_2). \quad (48)$$

Moreover, due to (48) and $c^2 - s^2 = 1$, the relation

$$\frac{1}{2}(\tilde{\mathcal{A}}_0 \cdot \mathbf{e}_1 \cdot \tilde{\mathcal{A}}_2 + \tilde{\mathcal{A}}_2 \cdot \mathbf{e}_1 \cdot \tilde{\mathcal{A}}_0) = \Xi_1\left(\frac{1}{2}(\mathcal{A}_0 \cdot \mathbf{e}_1 \cdot \bar{\mathcal{A}}_2 + \mathcal{A}_2 \cdot \mathbf{e}_1 \cdot \bar{\mathcal{A}}_0)\right) \quad (49)$$

holds. Consequently, the right-hand side of the equation (29) for the transformed data is equal to the transformed right-hand side of this equation for the original data. It follows that $\tilde{\mathcal{A}}_1 = \Xi_1(\mathcal{A}_1)$ and thus for the preimage $\tilde{\mathcal{A}}(t) = \Xi_1(\mathcal{A}(t))$, which implies (44).

In order to prove (45), it suffices to consider only the reflection Ξ_s with respect to the space-like plane spanned by \mathbf{e}_1 and \mathbf{e}_2 and the reflection Ξ_t with respect to the time-like plane spanned by \mathbf{e}_1 and \mathbf{e}_3 . Indeed, any other reflection with respect to a non-light-like plane containing the \mathbf{e}_1 axis can be obtained as a composition of Ξ_s or Ξ_t and two hyperbolic rotations about the \mathbf{e}_1 axis.

Similarly to the first part of the proof, we extend the mappings Ξ_s and Ξ_t from pure vectors to the whole Clifford algebra (excluding the last coordinate)

$$\begin{aligned} \Xi_s([a_0, \lambda, \mu, \nu, a_4, a_5, a_6, 0]) &= [-a_0, \lambda, \mu, -\nu, -a_4, a_5, a_6, 0], \\ \Xi_t([a_0, \lambda, \mu, \nu, a_4, a_5, a_6, 0]) &= [a_0, \lambda, -\mu, \nu, -a_4, -a_5, a_6, 0]. \end{aligned} \quad (50)$$

A direct computation confirms that the formulas (48) and (49) remain valid, provided that the control points of $\tilde{\mathcal{A}}(t)$ are constructed using the parameters $-\phi_0, -\phi_2$, while the control points of $\mathcal{A}(t)$ are constructed using the original parameters ϕ_0, ϕ_2 . \square

4.2 Standardized positions of the input data

In the remainder of this paper we assume that the sum $\mathbf{t}_0 + \mathbf{t}_1$ of the given boundary derivatives is a space-like vector. We need this assumption in order to define the standard position in a symmetric fashion. For instance, if the data are sampled from a space-like curve with some step size h , then this assumption is always satisfied provided that h is sufficiently small. Note that the medial axis transform of a planar domain is a system of curves in Minkowski space. The tangent vectors of these curves are never time-like, and only isolated boundary points with light-like tangents may be present.

Definition 2 *If $\mathbf{t}_0 + \mathbf{t}_1$ is a positive multiple of \mathbf{e}_1 and $\mathbf{p}_0 = \mathbf{0}$, then the input C^1 Hermite data are said to be in a **standard position**. We parameterize the main branch of MPH interpolants as follows. First, we transform the input data to a standard position. Then we construct the MPH interpolants $\mathbf{p}_0[\phi_0, \phi_2](t)$ of the main branch. Finally, we transform the solutions back to the original position. This parameterized family of MPH interpolants will be denoted by $\mathbf{s}[\phi_0, \phi_2](t)$*

Due to Lemma 8, this parameterization of the main branch of MPH interpolants is well defined, as the particular choice of a standard position does not

matter. The labeling of the solutions (i.e., the mapping $(\phi_0, \phi_2) \mapsto \mathbf{s}[\phi_0, \phi_2](\cdot)$) is invariant with respect to special Lorentz transforms, while reflections change the signs of both parameters ϕ_0, ϕ_2 . In addition we have the following result.

Proposition 9 *We consider the interpolants $\mathbf{s}[\phi_0, \phi_2](t)$ and $\tilde{\mathbf{s}}[\phi_0, \phi_2](t)$ of the input data $\mathbf{p}_0, \mathbf{p}_1, \mathbf{t}_0, \mathbf{t}_1$ and of the ‘reversed’ data $\tilde{\mathbf{p}}_0 = \mathbf{p}_1, \tilde{\mathbf{p}}_1 = \mathbf{p}_0, \tilde{\mathbf{t}}_0 = -\mathbf{t}_1, \tilde{\mathbf{t}}_1 = -\mathbf{t}_0$, respectively. Then the equation*

$$\forall t : \tilde{\mathbf{p}}[\phi_0, \phi_2](1 - t) = \mathbf{p}[-\phi_2, -\phi_0](t) \quad (51)$$

holds for all values of the parameters ϕ_0 and ϕ_2 .

Proof: We assume that the original data are already in a standard position. The reversed data is transformed into a standard position by a translation by the vector $-\mathbf{p}_1$ and a reflection with respect to the r axis, which can be decomposed into the reflection $\mathbf{c} \rightarrow -\mathbf{c}$ with respect to the origin and the reflection Ξ_{xy} with respect to the xy plane.

The standard positions associated with the given and reversed data are related by swapping \mathbf{t}_0 and \mathbf{t}_1 and by the reflection Ξ_{xy} . After taking the symmetry of the equations (28) and (29) with respect to \mathcal{A}_0 and \mathcal{A}_2 into account, the proof follows from the second part of Lemma 8. \square

Finally we apply these observations to the special case $\phi_0 = \phi_2 = 0$.

Theorem 10 *The interpolant $\mathbf{s}[0, 0](t)$ is invariant under translations and Lorentz transforms, and it is symmetric with respect to reversion of the data.*

In addition to these invariance properties, we show that this particular solution also possesses the optimal approximation order.

5 Approximation order

We assume that a sufficiently smooth (C^4) space-like curve $\mathbf{C}(T)$ in Minkowski space $\mathbb{R}^{2,1}$ is given. It may be a branch of the medial axis transform (MAT) of a planar domain. In this situation, the curve is space-like, except for those end points, which correspond to vertices (curvature maxima) of the boundary of the domain.

In order to approximate this curve by a quintic MPH spline, we sample C^1 Hermite boundary data from segments $T \in [t_0, t_0 + h]$ and apply the interpolation procedure. The next theorem analyzes the behavior of the error as the step size h tends to zero. As noted in [11], the results on the approximation

order of the MAT imply analogous results for the Hausdorff distance of the associated planar domains.

Theorem 11 *If the step-size h is sufficiently small, then the main branch of the interpolants as introduced in Definition 1 exists, i.e., the solutions for $i = k = 1$ are computed solely using (19). In particular, the interpolant $\mathbf{s}[0,0](t)$ has approximation order 4, and all other interpolants (for arbitrary but constant values of the free parameters $\bar{\phi}_0, \bar{\phi}_2$) have only approximation order 1.*

Proof: We prove this theorem using Taylor series. Without loss of generality we choose $\mathbf{C}(0) = (0, 0, 0)^\top$ and $\mathbf{C}'(0) = (1, 0, 0)^\top$, hence

$$\mathbf{C}(T) = \left(T + \sum_{i=2}^{\infty} \frac{x_i}{i!} T^i, \sum_{i=2}^{\infty} \frac{y_i}{i!} T^i, \sum_{i=2}^{\infty} \frac{r_i}{i!} T^i \right)^\top, \quad (52)$$

where x_i, y_i and r_i are arbitrary but fixed coefficients, $i = 2, 3, \dots$. The Hermite interpolation procedure is applied to the segment $\mathbf{c}(t) = \mathbf{C}(th)$, $t \in [0, 1]$, where the step-size h specifies the length.

In order to prove the Theorem, we evaluate the Taylor expansions with respect to h of all quantities occurring in the interpolation algorithm, using a suitable computer algebra tool. Due to the space limitations and the complexity of the expressions we present only the leading terms of certain quantities¹.

First we generate the Taylor expansions of the Hermite boundary data, $\mathbf{p}_0 = (0, 0, 0)^\top$, $\mathbf{t}_0 = (h, 0, 0)^\top$,

$$\mathbf{p}_1 = \begin{pmatrix} h + \frac{1}{2}x_2h^2 + \frac{1}{6}x_3h^3 + \dots \\ \frac{1}{2}y_2h^2 + \frac{1}{6}y_3h^3 + \dots \\ \frac{1}{2}r_2h^2 + \frac{1}{6}r_3h^3 + \dots \end{pmatrix}, \quad \mathbf{t}_1 = \begin{pmatrix} h + x_2h^2 + \frac{1}{2}x_3h^3 + \dots \\ y_2h^2 + \frac{1}{2}y_3h^3 + \dots \\ r_2h^2 + \frac{1}{2}r_3h^3 + \dots \end{pmatrix}.$$

In order to transform these data into a standard position, we apply a Lorentz transform with the Taylor expansion

$$U = \begin{pmatrix} 1 - \frac{y_2^2 - r_2^2}{8}h^2 + \dots & \frac{y_2}{2}h + \frac{y_3 - x_2y_2}{4}h^2 + \dots & -\frac{r_2}{2}h - \frac{r_3 - x_2r_2}{4}h^2 + \dots \\ -\frac{y_2}{2}h - \frac{y_3 - x_2y_2}{4}h^2 + \dots & 1 - \frac{y_2^2}{8}h^2 + \dots & 0 \\ -\frac{r_2}{2}h - \frac{r_3 - x_2r_2}{4}h^2 + \dots & -\frac{y_2r_2}{4}h^2 + \dots & 1 + \frac{r_2^2}{8}h^2 + \dots \end{pmatrix}.$$

The squared norms of the boundary derivatives are

$$\|\mathbf{t}_0\|^2 = \|U(\mathbf{t}_0)\|^2 = h^2, \quad \|\mathbf{t}_1\|^2 = \|U(\mathbf{t}_1)\|^2 = h^2 + 2x_2h^3 + \dots,$$

¹ The details of the computation (Maple worksheets) are available in electronic form at www.ag.jku.at/pubs/C1_MPH_Maple.tar.gz.

i.e., these vectors are space-like for sufficiently small h . Moreover, the quantities $\alpha(\mathbf{t}_0)$ and $\alpha(\mathbf{t}_1)$ (see Lemma 4) have the expansions

$$\alpha(\mathbf{t}_0) = 2h + \frac{1}{8}(r_2^2 - y_2^2)h^3 + \dots, \quad \alpha(\mathbf{t}_1) = 2h + 2x_2h^2 + \dots, \quad (53)$$

they are therefore positive for sufficiently small h . As the next step, we generate the Taylor expansions of the control points of the preimage curve. Using (19) we obtain $\mathcal{A}_0(\bar{\phi}_0)$ and $\mathcal{A}_2(\bar{\phi}_2)$. After substituting them into (29) one can verify that the right hand side R of the equation (29) satisfies

$$\alpha(R) = 10(9 + \cosh(\phi_2 - \phi_0))h + 5(9 + \cosh(\phi_2 - \phi_0))x_2h^2 \dots, \quad (54)$$

i.e., $\alpha(R)$ becomes positive as $h \rightarrow 0$. Consequently, for sufficiently small step-size h , the solutions are obtained solely by using (19).

We refrain from presenting the expansions of the preimage control points, as even the leading terms are rather complicated. Finally, after integration and transforming the results back from the standard position, we arrive at the Taylor expansion of the MPH interpolant $\mathbf{p}[\bar{\phi}_0, \bar{\phi}_2]$ and compare it with the given curve segment. We focus on the main branch of the interpolants. The leading term of the x coordinate of $\mathbf{s}[\phi_0, \phi_2](t)$ equals

$$\begin{aligned} & [t + \frac{1}{2}((\cosh \phi_0)\sqrt{10 \cosh(\phi_2 - \phi_0) + 90} - 3 \cosh(\phi_2 - \phi_0) - 7)t^2 \\ & - \frac{1}{2}((3 \cosh \phi_0 + \cosh \phi_2)\sqrt{10 \cosh(\phi_2 - \phi_0) + 90} - 12 \cosh(\phi_2 - \phi_0) - 28)t^3 \\ & + \frac{1}{2}((3 \cosh \phi_0 + 2 \cosh \phi_2)\sqrt{10 \cosh(\phi_2 - \phi_0) + 90} - 15 \cosh(\phi_2 - \phi_0) - 35)t^4 \\ & - \frac{1}{2}((3 \cosh \phi_0 + \cosh \phi_2)\sqrt{10 \cosh(\phi_2 - \phi_0) + 90} - 6 \cosh(\phi_2 - \phi_0) - 14)t^5]h. \end{aligned}$$

By comparing this expansion with the x -coordinate of $\mathbf{c}(t)$ we see that the convergence is better than linear if and only if the coefficients of t^2 , t^3 , t^4 and t^5 vanish. By solving the resulting equations it can be shown that this is the case if and only if $\phi_0 = \phi_2 = 0$. Moreover, the Taylor expansion of $\mathbf{s}[0, 0]$ matches the expansion of $\mathbf{c}(t)$ up to h^3 . Finally, by computing the expansions of the interpolants $\mathbf{p}[\bar{\phi}_0, \bar{\phi}_2]$ of the other branches, one can verify that for any values of $\phi_0, \phi_2 \in \mathbb{R}$ the approximation error converges to 0 as $\mathcal{O}(h^1)$ only. \square

Remark 12 For a fixed step-size h , the interpolant $\mathbf{s}[0, 0]$ is not necessarily the best possible one. It is a challenging problem to identify the optimal solution among the four two-parameter families of interpolants. In the case of C^1 interpolants in the Euclidean plane, this problem is now completely solved [3]. For PH quintics in the Euclidean space, [8] proposes to identify the best solution with the help of an integral shape measure. This technique could be adapted to the Minkowski case, possibly by restricting it to the first two components of the curve in $\mathbb{R}^{2,1}$, which represent the medial axis of the associated planar domain. A detailed discussion is beyond the scope of the present paper.

6 Examples

We illustrate the theoretical results by several examples.

Example 1 We apply the C^1 Hermite interpolation scheme to the data

$$\mathbf{p}_0 = (0, 0, 0)^\top, \quad \mathbf{p}_1 = (0, 1, 0)^\top, \quad \mathbf{t}_0 = (3, 0, 0)^\top, \quad \mathbf{t}_1 = (3, 0, 0)^\top. \quad (55)$$

Note that these data lie in a space-like plane. As a natural question, one may ask for the planar curves among all interpolants. We present the following results, without giving a proof: Let the input data lie in a plane π and let $\mathbf{t}_0 + \mathbf{t}_1$ be a space-like vector.

- If the plane π is space- or light-like, then the four interpolants $\mathbf{p}[(i, 0), (k, 0)]$, $i, k \in \{1, 2\}$ are planar.
- If the plane π is time-like, then the interpolation scheme gives 16 planar interpolants $\mathbf{p}[(i, 0), (k, 0)]$, $i, k \in \{1, 2, 3, 4\}$.

Consequently, the ‘best’ solution $\mathbf{s}[0, 0](t)$ has the additional advantage of *preserving planarity*.

Figure 1a shows the four planar interpolants to the given data (55). As the data lie in the space-like plane $x_3 = 0$, these four curves are identical to the solutions of the C^1 Hermite interpolation problem in the Euclidean plane, see [3,7]. Note that the interpolant $\mathbf{p}[0, 0]$ (bold) is the ‘best’ one. In order to illustrate the influence of the free parameters ϕ_0 and ϕ_2 , Figure 1b shows the interpolants $\mathbf{p}[\phi_0, \phi_2]$, where $\phi_0 = \phi_2 = \frac{l}{3}$, $l = -6, \dots, 6$.

Example 2 The interpolation algorithm and Theorem 11 allow to approximate any space-like C^∞ curve $\mathbf{c}(t)$ by a quintic MPH spline. Let the parameter domain of $\mathbf{c}(t)$ be $[0, 1]$. Using binary subdivision, we split the interval into 2^n segments. For each segment we construct the MPH interpolant $\mathbf{s}[0, 0]$. If the error is not sufficiently small, then we continue in subdividing. Clearly, using an adaptive subdivision reduces the number of interpolants. Due to Theorem 11, the error converges to 0 as $\mathcal{O}(16^{-n})$.

We demonstrate the order of convergence by the following example, see Figure 2. Consider the segment of the C^∞ curve

$$\mathbf{c}(t) = (1.2t, 0.25t \sin(10t - 1), 1 - \frac{\cosh(t - \frac{1}{2})}{\cosh \frac{1}{2}})^\top; \quad t \in [0, 1]. \quad (56)$$

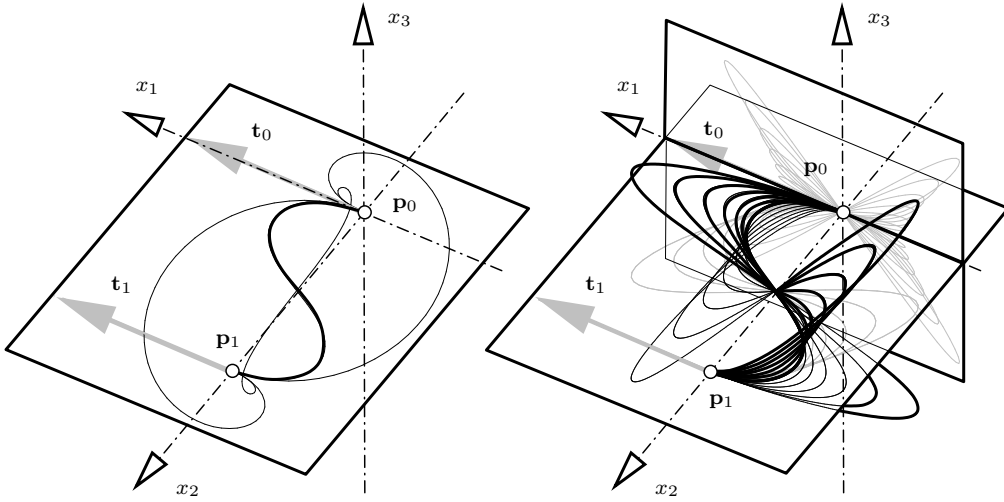


Fig. 1. a) The four planar MPH interpolants to given planar input data, and b) the family of MPH interpolants $\mathbf{p}[\phi_0, \phi_2]$ for various values of ϕ_0 and ϕ_2 . The projections of the interpolants into the x_1x_2 - and x_1x_3 -plane are shown in grey.

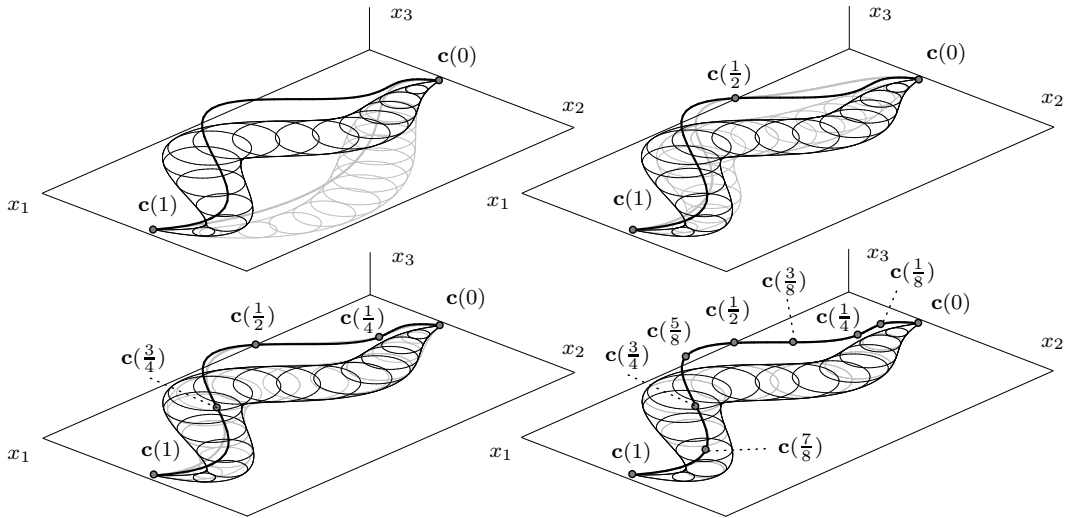


Fig. 2. Approximation of a C^∞ curve (black) by an MPH quintic spline (gray) obtained by splitting the parameter domain into 1, 2, 4, and 8 spans. The segment boundaries are indicated by the small circles. In the last case, the curves are almost indistinguishable. In addition to the curve in $\mathbb{R}^{2,1}$, the figure shows the corresponding one-parameter families of circles and their envelopes in the x_1x_2 -plane. The curve in $\mathbb{R}^{2,1}$ is the medial axis transform (MAT) of the planar domain which is bounded by the two envelopes.

The approximation error (sample-based estimation) and its improvement on the first interval span in each step of subdivision are reported in Table 1. The ratios of adjacent errors tend to 16, as predicted by the approximation order.

Table 1

Numerical results obtained by uniform refinement.

no. segments	error	ratio	no. segments	error	ratio
1	$4.752 \cdot 10^{-1}$	–	64	$1.066 \cdot 10^{-7}$	17.87
2	$7.020 \cdot 10^{-2}$	6.78	128	$6.244 \cdot 10^{-9}$	17.07
4	$7.603 \cdot 10^{-3}$	9.23	256	$3.769 \cdot 10^{-10}$	16.57
8	$6.429 \cdot 10^{-4}$	11.83	512	$2.314 \cdot 10^{-11}$	16.29
16	$3.572 \cdot 10^{-5}$	18.00	1024	$1.433 \cdot 10^{-12}$	16.15
32	$1.905 \cdot 10^{-6}$	18.75	2048	$8.913 \cdot 10^{-14}$	16.07

Table 2

Numerical results obtained for a curve with a light-like tangent vector.

no. segments	error	ratio	no. segments	error	ratio
1	$7.450 \cdot 10^{-2}$		8	$9.934 \cdot 10^{-4}$	3.99
2	$1.593 \cdot 10^{-2}$	4.68	16	$2.487 \cdot 10^{-4}$	3.99
4	$3.966 \cdot 10^{-3}$	4.02	32	$6.222 \cdot 10^{-5}$	4.00

Example 3 Finally we consider the case of light-like tangent vectors, which has been excluded so far. Since light-like curves do not occur as medial axis transforms, we consider a curve segment which has a light-like boundary tangent at its start point, while all other tangents are space-like. For instance, this situation occurs at those end points of the medial axis transforms which correspond to vertices of the boundary curve.

We consider the segment of the C^∞ curve

$$\mathbf{c}(t) = (1.15t - \sqrt{2}, (1.15t - \sqrt{2})^2, \frac{1}{2}(1.15t - \sqrt{2})^3 + 1.7)^\top, \quad t \in [0, 1], \quad (57)$$

which has a light-like tangent at $t = 0$. Analogously to the previous example, Table 2 shows the approximation error and its improvement.

The theoretical analysis of this case led to challenging problems of symbolic formula manipulation. Following our numerous numerical experiments (cf. Table 2), we were inclined to formulate the

Conjecture 1 *The approximation order at points with light-like tangents is equal to two for the four interpolants $\mathbf{p}[(i, 0), (k, 0)](t)$, $i, k \in \{1, 4\}$. For all other interpolants, the approximation order is equal to one.*

7 Conclusion

As observed in [4,13], MPH curves are well suited for approximating the medial axis transform of a planar domain, since they provide a rational parameterization of the domain boundaries and of its offset curves. According to [5], MPH curves can be generated with the help of a closed form representation using

the Clifford algebra $\mathcal{C}(2, 1)$. Based on these earlier results, we presented a general method for approximating any space-like C^∞ curve by a C^1 MPH quintic spline. With the help of asymptotic analysis we proved that the approximation order is equal to four. The method is superior to the G^1 interpolation algorithm, as the solvability does not depend on the input data and the approximation order is not reduced to two at Minkowski inflections.

Acknowledgment The authors were supported by the Austrian Science Fund (FWF), project no. P17387-N12. They wish to thank the anonymous reviewers for their comments which have helped to improve the paper.

References

- [1] Cho H. Ch., Choi, H. I., Kwon S.-H., Lee D. S., and Wee N.-S., Clifford algebra, Lorentzian geometry and rational parametrization of canal surfaces, *Comp. Aided Geom. Design*, 21 (2004), 327–339.
- [2] Choi, H. I., Choi, S. W., and Moon, H. P., Mathematical theory of medial axis transform, *Pacific J. Math.*, 181(1) (1997), 57–88.
- [3] Choi, H. I., Farouki, R. T., Kwon, S.-H., Moon, H. P., Topological Criterion for Selection of Quintic Pythagorean-Hodograph Hermite Interpolants. *Comput. Aided Geom. Design*, to appear.
- [4] Choi, H. I., Han, Ch. Y., Moon, H. P., Roh, K. H., and Wee, N. S., Medial axis transform and offset curves by Minkowski Pythagorean hodograph curves, *Comp.-Aided Design*, 31 (1999), 59–72.
- [5] Choi, H. I., Lee, D. S., and Moon, H. P., Clifford algebra, spin representation and rational parameterization of curves and surfaces, *Advances in Computational Mathematics*, 17 (2002), 5–48.
- [6] Degen, W. L. F., Exploiting curvatures to compute the medial axis for domains with smooth boundary, *Comp. Aided Geom. Design*, 21 (2004), 641–660.
- [7] Farouki, R. T., Pythagorean-hodograph curves, *Handbook of Computer Aided Geometric Design* (J. Hoschek, G. Farin and M.-S. Kim, eds.), Elsevier, 2002, 405–427.
- [8] Farouki, R. T., al-Kandari, M., and Sakkalis, T, Hermite interpolation by rotation-invariant spatial Pythagorean-hodograph curves, *Advances in Computational Mathematics*, 17 (2002), 369–383.
- [9] Farouki, R. T., and Sakkalis T., Pythagorean hodographs, *IBM Journal of Research and Development*, 34 (1990), 736–752.
- [10] Jüttler, B., and Mäurer, C., Cubic Pythagorean Hodograph Spline Curves and Applications to Sweep Surface Modeling, *Comp.-Aided Design*, 31 (1999), 73–83.
- [11] Kosinka, J., and Jüttler, B., G^1 Hermite Interpolation by Minkowski Pythagorean Hodograph Cubics, *Comp. Aided Geom. Des.*, 23 (2006), 401–418.

- [12] Kim, G.-I., and Ahn M.-H., C^1 Hermite interpolation using MPH quartic, *Comp. Aided Geom. Design*, 20 (2003), 469–492.
- [13] Moon, H. P., Minkowski Pythagorean hodographs, *Comp. Aided Geom. Design*, 16 (1999), 739–753.
- [14] Pottmann, H., and Peternell, M., Applications of Laguerre geometry in CAGD. *Comp. Aided Geom. Design*, 15 (1997), 165–186.
- [15] Rowland, T., and Weisstein, E., Clifford Algebra. From MathWorld—A Wolfram Web Resource. <http://mathworld.wolfram.com/CliffordAlgebra.html>
- [16] Šír, Z., and Jüttler, B., Spatial Pythagorean Hodograph Quintics and the Approximation of Pipe Surfaces, *The Mathematics of Surfaces XI*, Springer Lecture Notes on Computer Science vol. 3604, Berlin, 2005, 364–380.
- [17] Šír, Z., and Jüttler, B., C^2 Hermite interpolation by spatial Pythagorean hodograph curves, *Math. Comp.*, 76 (2007), 1373–1391.